Development of stackedporous tantalum oxide layers by anodization

L. Fialho*[1], C. F. Almeida Alves[2], L. S. Marques[3], S. Carvalho[1,4]

[1]CFUM-UP, Physics Department, University of Minho, 4800-058 Guimarães, Portugal

[2]INL - International Iberian Nanotechnology Laboratory, Av. Mestre José Veiga s/n, 4715-330 Braga, Portugal

[3]CFUM-UP, Physics Department, University of Minho, Campus of Gualtar, 4710-057 Braga, Portugal

[4]SEG-CEMMPRE Mechanical Engineering Department, University of Coimbra, 3030-788 Coimbra

Abstract

Nanoporous tantalum oxide (Ta_2O_5) attraction has been increasing due its high variety of applications, from protective coatings, photocatalysts to biomedical devices. Anodization is a surface modification technique, inexpensive, versatile and easily scalable, widely used to produce these nanostructures. In this work, Ta_2O_5 nanoporous surface were produced by anodization in a non-aqueous HF-free electrolyte composed by ethylene glycol, water and ammonium fluoride (NH_4F), for different anodization parameters (electrolyte concentration, applied potential and time) and comparing a two-step with one-step anodization process. The surface morphology of each sample was investigated by scanning electron microscopy (SEM) and the sample with the optimized nanostructure was characterized in terms of cross-section morphology, chemical composition and crystalline structure. The concentration of NH_4F and applied potential demonstrated a

---

* *Email address:* luisa.gfialho@gmail.com (L. Fialho)

significant impact on current-density-time curve profile, and thereafter in surface morphology, when comparing with the increase of process duration. The optimized nanoporous surfaces were formed under strong electrochemical conditions inducing an increase in both current density and electrolyte temperature and exhibit a morphology consisting in multiple thin porous layers. which is of great interest for photocatalyst application. Chemical analysis identified an high content of O after anodization and detected the presence F, which is consistent with an amorphous Ta_2O_5 layer with fluoride ions incorporation. Thereby, control the electrochemical conditions is crucial to control the morphology of Ta_2O_5.

1. Introduction

Nowadays, surface modification is widely used to functionalize and strategically enhance the material surface properties. The surface modification can be broadly qualified either as addiction or removing material or as changing its chemical composition and/ or topography [1]. Those treatments can be achieved by methods that can be classified into three categories: mechanical, physical and chemical surface modifications. The most common mechanical modification procedures have typically as a goal the achievement of specific topography or roughness, minimize surface contamination and improve adhesion in the following bonding steps. This category includes grinding, matching, polishing or blasting. In physical treatments, (as examples thermal spraying, physical vapor deposition, ion implantation and deposition) and in chemical modifications (which encloses chemical, electrochemical treatments, sol-gel process, chemical vapor deposition and biochemical modification) the main goal is to control the physical properties, increase protection surface and in some cases add new functionalities [1], [2].

The anodic oxidation, also called as anodization, is an electrochemical, low-cost and easily scale-up method [3], [4], which operates as an electrochemical cell. A potential is applied between the anode (metallic surface) and the cathode (counter electrode such as graphite, platinum, lead), transferring charges and ions and a subsequently an oxide layer is formed. This process allows the production of a controllable thickness of the protective and compact oxide layer [5]. Moreover, depending on the process parameters, anodization can modify the roughness in order to obtain micro/nano-porous or controlled nanotubular structures besides chemical surface modification [6]–[8]. Working in potentiostatic mode, the electrolyte composition and concentration, the temperature, the applied potential and the process duration are adjusted according to the desired morphology, physical and chemical properties [1], [6], [9], [10].

The most studied anodized metal is aluminum (Al) and the growth of self-ordered porous alumina layers [4] by two-step anodization was proposed by Masuda and Fukuda [11]. More recently, well-ordered nanoporous or nanotubular structures, under optimized electrochemical conditions, has been reported for other valve metals, like titanium (Ti), zirconium (Zr), niobium (Nb), tungsten (W) and tantalum (Ta) [4], [12]. Hence, those metals have becoming more attractive due to their potential use as catalysts, catalysts supports for fuel, waveguides, biological purposes, photoelectrochemical applications, among others [13]. For some applications, it is important that the anodic layer exhibits a porous or tubular structure. Nanostructures can be achieved in alumina using an electrolyte composed sulfuric acid (H_2SO_4) or phosphoric acid (H_3PO_4) [14]. On the other hand, in some valve metals, such as Zr, Ti and Ta, it is necessary the presence of fluoride ions (F^-) in the electrolyte because the nanostructures grow as a result of competition between electrochemical oxide formation and the chemical dissolution of oxide by F^- ions [1], [4], [8], [15], [16].

Additionally, Fu et al. [17] showed a research trend about "titania nanotubes by anodization method" showing more than 200 publications per year in the past 7 years. Regarding to biomedical applications, researchers have been paying more attention to Ti and its alloys [1] due to the fact that about 40% of currently implant materials are based on those metals [12], and therefore, in this context, the majority of literature about anodization involve these metals and alloys [18]. Anodized Tantala is typically used in capacitors and as protective coating material for chemical equipment (e.g. optical devices) [19], but is also used in medical devices due to its enhanced bioactivity [20]–[23]. In addition, due to its excellent dielectric properties, it seems to be also an excellent option in electronic and sensor devices [19], [24], [25]. The most part of the literature has studied anodizing Ta using electrolytes composed by a mixture of hydrofluoric acid (HF) and H_2SO_4 [13], [19], [26]–[29] to obtain nanoporous surfaces, with very few studies focusing on Ta anodization in acid free eletrolytes.Allam et al. [30] published the first study dedicated to the effect of additives, as H_3PO_4, ethylene glycol (EG) or dimethyl sulfoxide (DMSO), in aqueous electrolyte mixture containing HF and H_2SO_4 resulting on Ta_2O_5 nanotube arrays, vertically orientated. Later, El-Sayed et al. [31] demonstrated that the addition of 10 wt.% EG to the acid mixture allowed a stable formation of Ta_2O_5 nanotubes. On the other hand, Ta anodization in non-aqueous electrolyte combining glycerol and small concentration of ammonium fluoride (NH_4F) was investigated by Wei et al. [24], demonstrating the influence of the applied potential, fluoride concentration and water content in the electrolyte on the layer porosity. More recently, Momeni et al. [32] showed that glycerol containing NH_4F electrolyte produced an irregular porous film, while the mixture of glycerol and EG containing NH_4F can produce a highly ordered nanoporous surface [25], [33], which was not observed on EG electrolyte [25].. Yu et al. [34] reported for the first time the production nanoporous Ta_2O_5 with a coral-like

morphology using a mixture of EG, H_3PO_4, NH_4F and water. Uniform ordered Ta_2O_5 nanoporous were also obtained using a fluoride-free electrolyte, composed by glycerol and dipotassium phosphate, held at 180°C [35].

In order to achieve well-ordered nanoporous structure, an optimized second anodization step has been considered crucial to improve the surface morphology of TiO_2 [12]. In this two-step anodization approach, the first step creates a nano-pattern of ordered nano-dimples which serves as a template for the growth of nanotubular surface in the second step [15]. Researchers demonstrated that this two-step treatment helps to avoid mechanical damage and improve structural uniformity of the nanotubes [17]. Nevertheless, it was only found one report using two-step anodization in an aqueous mixture of H2SO4 and HF with 5% EG to form NTs on Ta2O5 film previously deposited on Ti-Al-4V alloy by physical vapor deposition [36]. However, the authors did not discuss the impact of this methodology on the final morphology. Ta two-step anodization in HF-free electrolyte is thus still missing.

In the present work, it was explored the anodization process using a non-aqueous acid-free electrolyte composed by EG, 3 vol.% water and different content of NH_4F in a range of applied potentials with the purpose of develop nanostructured Ta anodic layer. In addition, one-step and two-step anodization were performed and compared regarding the improvement on the nanostructure. The morphology patterns were studied, in terms of the top-view and cross-section morphology, chemical composition and phase composition.

2. Materials and methods

2.1. Surface pre-treatment

Squares of high-pure tantalum sheet (99.95%) (Testbourne Lda) of 400mm^2 and 0.5 mm thickness were used as substrates in this study and called as Ta. Firstly, the samples were

ground with a series of silicon carbide (SiC) sandpapers such as P500, P800, P1200 and P2500 (CarbimetTM, Buehler), followed by polishing cloth with diamond paste (Diamond Suspension 3 and 6 µm, Struers) mixed with lubricant fluid (DP-Lubricant Blue, Struers) until achieve a mirror finishing with a mean roughness of 5 nm. Finally, all samples were ultrasonically cleaned in acetone for 15 min, 10 min in ethanol and 5 min in distilled (DI) water. Afterwards, an electropolishing was performed to smooth the samples surface (mean roughness of 3.7 nm) using a two-electrodes set-up where a Ta sample and graphite rod served as the working and counter electrodes, respectively, with 1.8 cm^2 area exposed to 1M H_2SO_4 (Sulfuric Acid 98%, Biochem, Chemopharma). Both electrodes were connected to a DC power supply (Agilent Technologies N5751A, 300V/2.5A/750W, LXI, USA). A constant voltage of 25V was applied for 10 min between both electrodes with a working distance of 3 cm. The electrolyte was continuously stirred at room temperature (RT). These samples were called by Ta-pol.

2.2. Development and optimization of the nanostructure

The nanostructures were obtained by anodization using the two-electrodes set-up previously described. Ta-pol samples were used as working electrodes while graphite rod was used as counter electrode. Both electrodes were immersed in an electrolyte constituted by EG (Ethylene Glycol anhydrous 99.8%, Sigma-Aldrich), 3 vol.% DI water and a variable amount NH_4F (Ammonium Fluoride 98%, Sigma-Aldrich). For result presentation purposes, the solvent mixture of EG and DI water was named as ES. The distance between the working and counter electrodes was fixed to 1.5 cm. The applied potential used was 40 or 60 V from 20 to 60 minutes. Also, two-step anodization was performed, with both steps carried out under the same conditions: 60V for 60 minutes using the same electrolyte. The process was stopped for 20 minutes before begining the second step. At the end of this procedure, surfaces were gently rinsed with DI water and

dried at room temperature. Anodized samples were named as Ta-anod*x* (*x* =1,2,3, … 7) and the detailed anodizing parameters are shown in Table 1~~Table 1~~.

2.3. Surface characterization

The morphology of Ta sheet, Ta-pol and Ta-anod*x* surfaces were analyzed by Field Emission Gun Scanning Electron Microscopy (FEGSEM) (Nova NanoSEM 200 microscope, FEI, USA) operating at 5kV in secondary electron mode. The samples were put on an aluminum stub with double sided carbon tape and then, by sputtering (208HR, Cressington), the samples were coated by an Au/Pd film with 1.5 nm of thickness. A Zeiss Crossbeam (Auriga Compact) equipped with Focus Ion Beam (FIB) and SEM was used to analysis their cross-section and thickness of the anodic layer. FIB cross-sections were performed on optimized anodic sample using a range of ion currents from 10 µA down to 200 pA and beam energy of 30 kV. Lower beam currents were used for the low-kV cleaning (200 pA). Anodic layer thickness was estimated by *ImageJ*.

Chemical composition of the Ta-pol and optimized anodic surfaces was qualitatively evaluated by Energy-dispersive X-ray Spectroscopy (EDS) using the EDAX-Pegasus X4M spectrometer (EDAX, USA) incorporated into the FEGSEM system, operating at 10 kV. Additional chemical characterization was carried out by using X-ray Photoelectron Spectroscopy (XPS) using a Kratos AXIS Ultra HSA, with VISION software for data acquisition and CASAXPS software for data analysis. The analysis was carried out with a monochromatic Al Kα X-ray source (1486.7 eV), operating at 15kV (150 W), in FAT mode (Fixed Analyzer Transmission), with a pass energy of 80 eV for survey and 40 eV for elemental spectrum. The effect of the electric charge was corrected by the reference of the carbon peak (285 eV).

X-ray diffraction (XRD) (Bruker D8 Discover, Germany) analysis was performed using 40 kV and 40 mA, with Cu radiation Kα radiation (λKα1=1.5406 Å and λKα2=1.54439

Å). The experiments were carried out in grazing angle geometry (3°). All the tests were performed with a step size of 0.04° and time per step of 1s, and 2θ range of 10-130°.

3. Results and discussion

3.1. Effect of electrochemical conditions on the Ta surface morphology

The Ta substrates (Figure 1~~Figure 1~~-a) used for the nanostructure growth were pre-treated by mechanical polishing and after electropolishing (Figure 1~~Figure 1~~-b) to get a more uniform and smooth surface with a compact oxide to perform the following electrochemical process (see inset on the Figure 1~~Figure 1~~-b a compact oxide around 1.5 µm of thickness). In fact, it should be noted that the Ta oxide formed in pre-treatment, Ta-pol sample, was compact, Figure 1~~Figure 1~~-b (inset), which become difficult to attack the oxide surface being necessary stronger anodizing conditions (higher potentials and/or more concentrated electrolytes) comparing with literature to be possible to dissolve/pitting it.
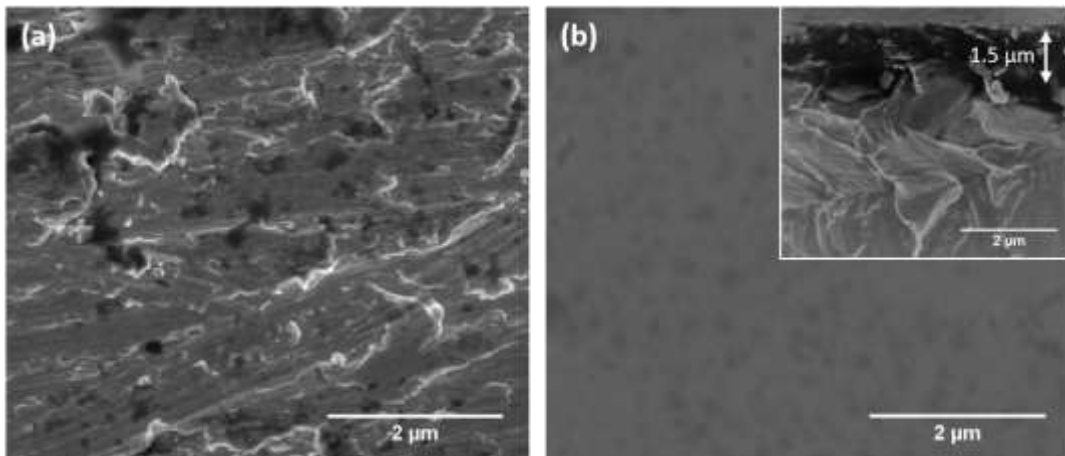

Figure 1. Top-view FEGSEM micrographs of (a) Ta sheet and (b) Ta polished surface after pre-treatment, Ta-pol sample, with cross-section FEGSEM view inset.

One-step anodization was performed at 40V using an electrolyte of 2.4wt.% NH$_4$F in ES for 20 minutes (Ta-anod1 in Table 1~~Table 1~~). The current density-curve can provide further information about the surface morphology evolution during the anodizing treatment [31]. The recorded current density-time curve under these conditions, Figure

2Figure 2-a, shows a initial decaying stage followed by a gradual increase with time until

the end of the procedure. As observed in Figure 3Figure 3-a (a1 and a2), a compact anodic

layer with few isolated small diameter pores was achieved.

Table 1. Anodizing parameters: applied potential, electrolyte (composition and concentration) and process duration.

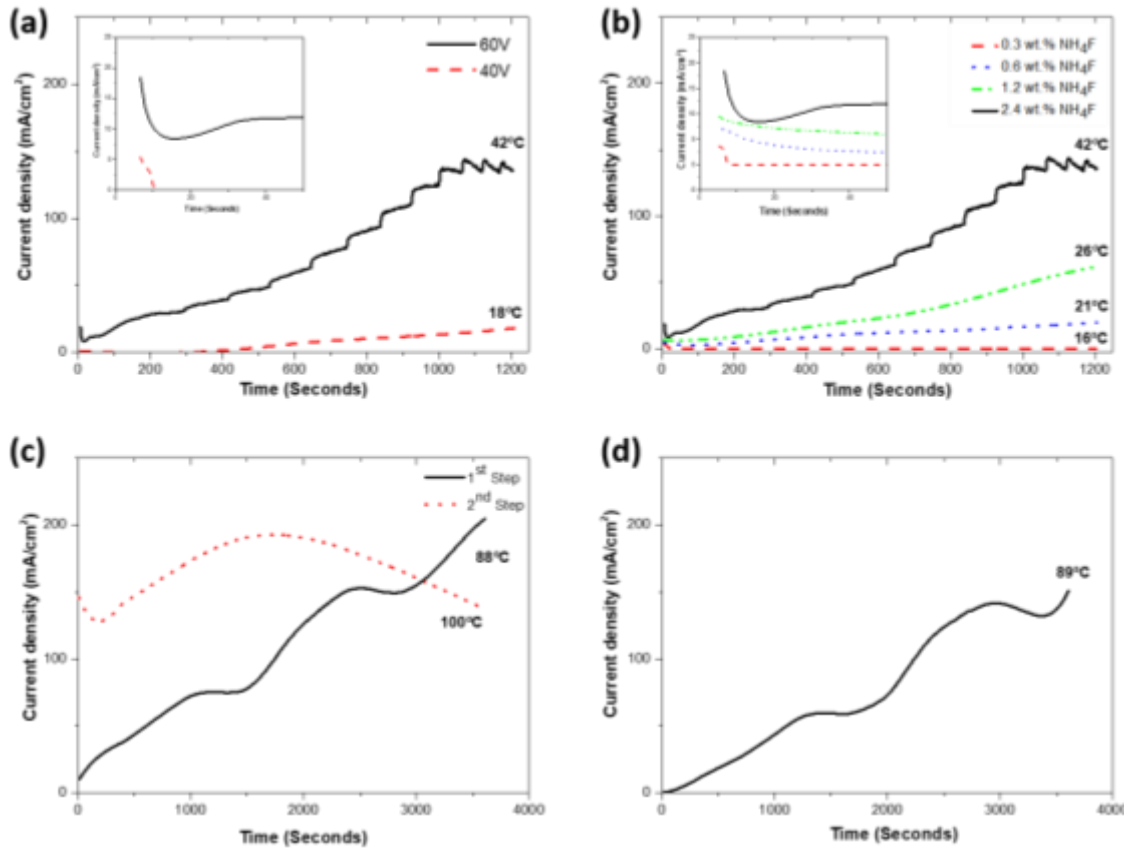| Sample	Anodization approach	Potential (V)	Electrolyte	Duration
Ta-anod1	1-step	40	2.4 wt.% NH_4F + ES	20 min
Ta-anod2	1-step	60	0.3 wt.% NH_4F + ES	20 min
Ta-anod3	1-step	60	0.6 wt.% NH_4F + ES	20 min
Ta-anod4	1-step	60	1.2 wt.% NH_4F + ES	20 min
Ta-anod5	2-step	60	1.2 wt.% NH_4F + ES	60 min (20 min stop) plus 60 min
Ta-anod6	1-step	60	1.2 wt.% NH_4F + ES	60 min
Ta-anod7	1-step	60	2.4 wt.% NH_4F + ES	20 min

Figure 2. Current density-time curves of several anodization assays: (a) Ta-anod1 and Ta-anod7 samples, (b) Ta-anod2, Ta-anod3, Ta-anod4 and Ta-anod7, (c) Ta- anod5 obtained by two-step and (d) Ta-anod6 obtained by one-step anodization under the same conditions. The electrolyte temperature recorded at the end of each anodization process is represented close to the respective curve. Inset images on (a) and (b) display the initial current density-time curve.
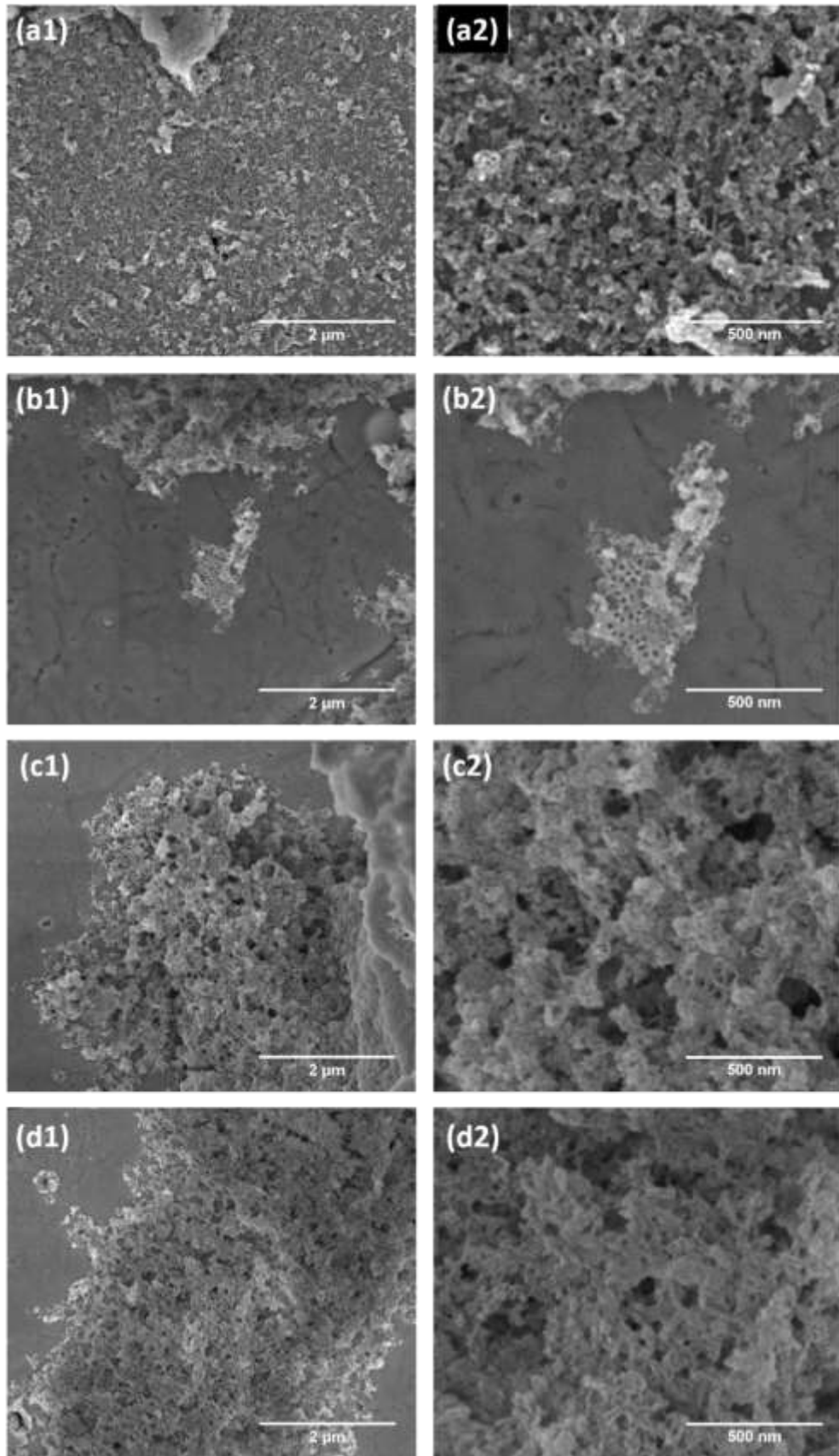
Figure 3.Top-view FEGSEM micrographs for Ta anodized samples at 60V for 20 min using an electrolyte solution with mixture of SE and (a) 2.4 wt.% NH$_4$F (Ta-anod1) at 40 V, (b) 0.3 wt.% NH$_4$F (Ta-anod2), (c) 0.6 wt.% NH$_4$F (Ta-anod3) and (d) 1.2 wt.% NH$_4$F ((Ta-anod4) at 60V for 20 min. (a1, b1, c1, d1): surface morphology of anodized samples and (a2, b2, c2, d2) their respectively high magnification.

Typically, three stages can be identified in the current density curve, Figure 4Figure 4.

First, an initial exponential decay related to the build-up of a resistive compact oxide layer

through Ta hydrolysis at the electrolyte/metal interface, according to Eq. 1. The current

density reaches a minimum value, which is believed to reflect the onset of electric field-

enhanced dissolution of oxide film, leading to the generation of the first small pores

(Figure 4Figure 4-stage I). This stage is followed by an increase of current as the surface

area increases when the pores extend and multiply due to the high dissolution rate of

Ta_2O_5 in fluoride-containing solutions, according to Eq. 2 [13], Figure 4Figure 4-stage II.

Finally, in the last stage it reaches a steady value [24], indicatinging that the oxide

formation and dissolution reactions are in equilibrium [4], [37].

$$2Ta + 5H_2O \rightarrow Ta_2O_5 + 10H^+ + 10e^- \tag{1}$$

$$Ta_2O_5 + 14F^- + 10H^+ \rightarrow 2[TaF_7]^{2-} + H_2O \tag{2}$$
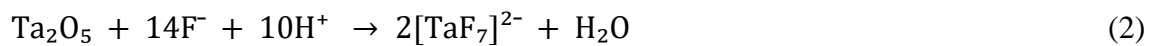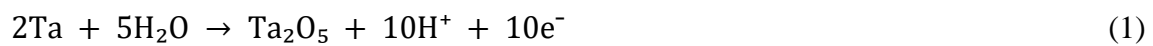
Several authors attribute to this third stage different meanings: a decrease in current

density with time indicates stable nanotubular or porous Ta oxide formation, as illustrated

inFigure 4Figure 4-stage III-ii, whereas a steady-state current or very slow increase is

related to the oxide nanotubes instability resulting in Ta dimpled surface morphology,

Figure 4Figure 4 stage III-i [31]. On the other hand, El-Sayed et al. [13] proposed a new

interpretation of current-time data, showing that pores are already formed in the first few

milliseconds of anodization. In our case, the current density slightly increased at the

second stage never reaching the third stage, and neither pore nor dimple development
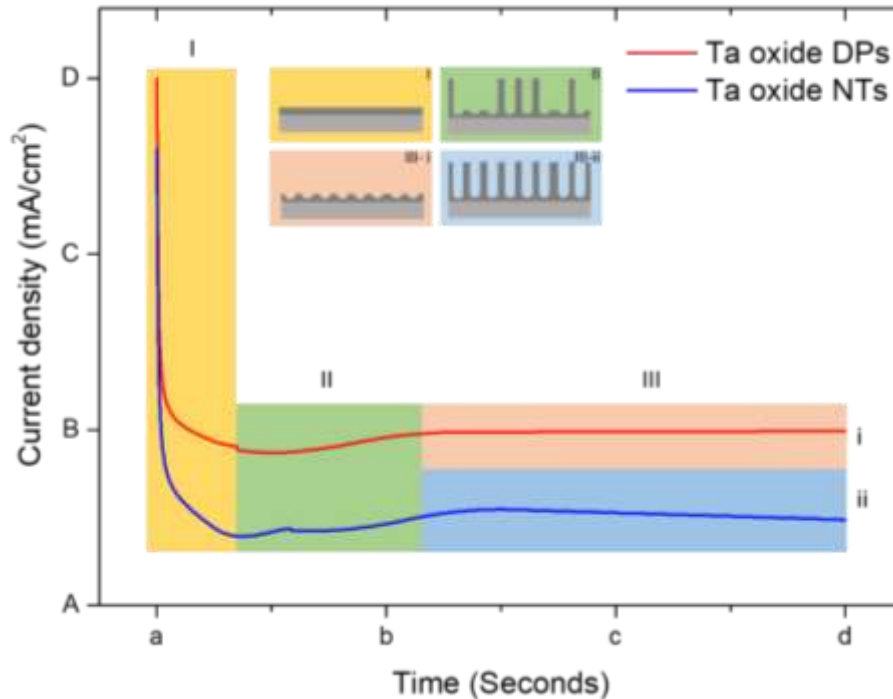
was observed.

Figure 4. Illustration of current density-time response during Ta anodization with the typical three stages: I) compact oxide layer formation, II) pores formation and extension, III) steady-state with i) dimples (DP) formation or ii) nanotubes (NTs) formation. Based on [31].

As the formation of pores could be enhanced by the applied electric field for anodization [19] and that an increase of the applied potential could provide a uniform porous distribution across the surface [38], the potential was raised from 40 to 60V for different NH_4F concentrations. In order to prevent current-density increase at the second stage, which is associated with nanotubes instability, and have a more controllable process, the amount of NH_4F on the electrolyte was kept at 0.3 wt.% (Ta-anod2 in Table 1Table 1). Under these conditions, only two stages were registered in current density-time curve: a drop of current density and a long steady-state, Figure 2Figure 2-b. This current density-time curve behavior was characteristic of formation of compact oxide in fluoride-free electrolytes [12]. Nevertheless, the morphology obtained presented small islands of oxide with tiny pits above the compact oxide layer, Figure 3Figure 3-b (b1 and b2), due to low fluoride ions concentration on the electrolyte and consequently a low dissolution rate.

Therefore, the NH$_4$F amount was increased to 0.6 wt.% (Ta-anod3 in Table 1Table 1), however this concentration was still not enough to form a homogenous porous anodic layer, Figure 3Figure 3-c (c1 and c2). Once again, the obtained morphologies indicate that the balance between oxidation and dissolution rate are not favorable, creating an irregular oxide layer with a few evidences of pore formation. When NH$_4$F content reached 1.2 wt.% (Ta-anod4), the curve tended to increase promptly with time, Figure 2Figure 2-b, however no ordered nanostructured oxide layer was achieved, Figure 3Figure 3-d (d1 and d2).

Two-step anodization is recommended in the literature as a better approach to reach well-ordered nanostructures, since the first step will create nucleation spots by the growth of pores that will induce, afterwards, on the second step the growth of well-ordered pores or tubes [12]. Thus, with the purpose to achieve a more uniform and homogeneous nanostructure, the previous hypothesis was tested (Ta-anod5 in Table 1Table 1). In order to enhance the nanopores development, the anodization time was increased to 60 min. As seen in Figure 5Figure 5-a (a1 and a2), the nanostructures developed under two-step anodization did not exhibit a uniform and well-ordered structure, but some pores were formed. Lower magnifications, Figure 5Figure 5-a1, show the presence of cracks and overlapping layers. This non-uniform morphology could be related to the abnormal current density behavior, Figure 2Figure 2-c. In the case ofMultilayered titania nanotubes formation using a two-step anodization by switching voltage from high to low (from the first to second step), neither cracks nor overlapping layers were reported [39]. Thus, to confirm this hypothesis, Ta one-step anodization was performed under the same parameters (sample Ta-anod6 in Table 1Table 1). As shown in Figure 5Figure 5-b (b1 and b2), the overall morphology of the anodic layer was quite improved exhibiting a more

uniform surface and no cracks. However, a bimodal porosity was achieved with some
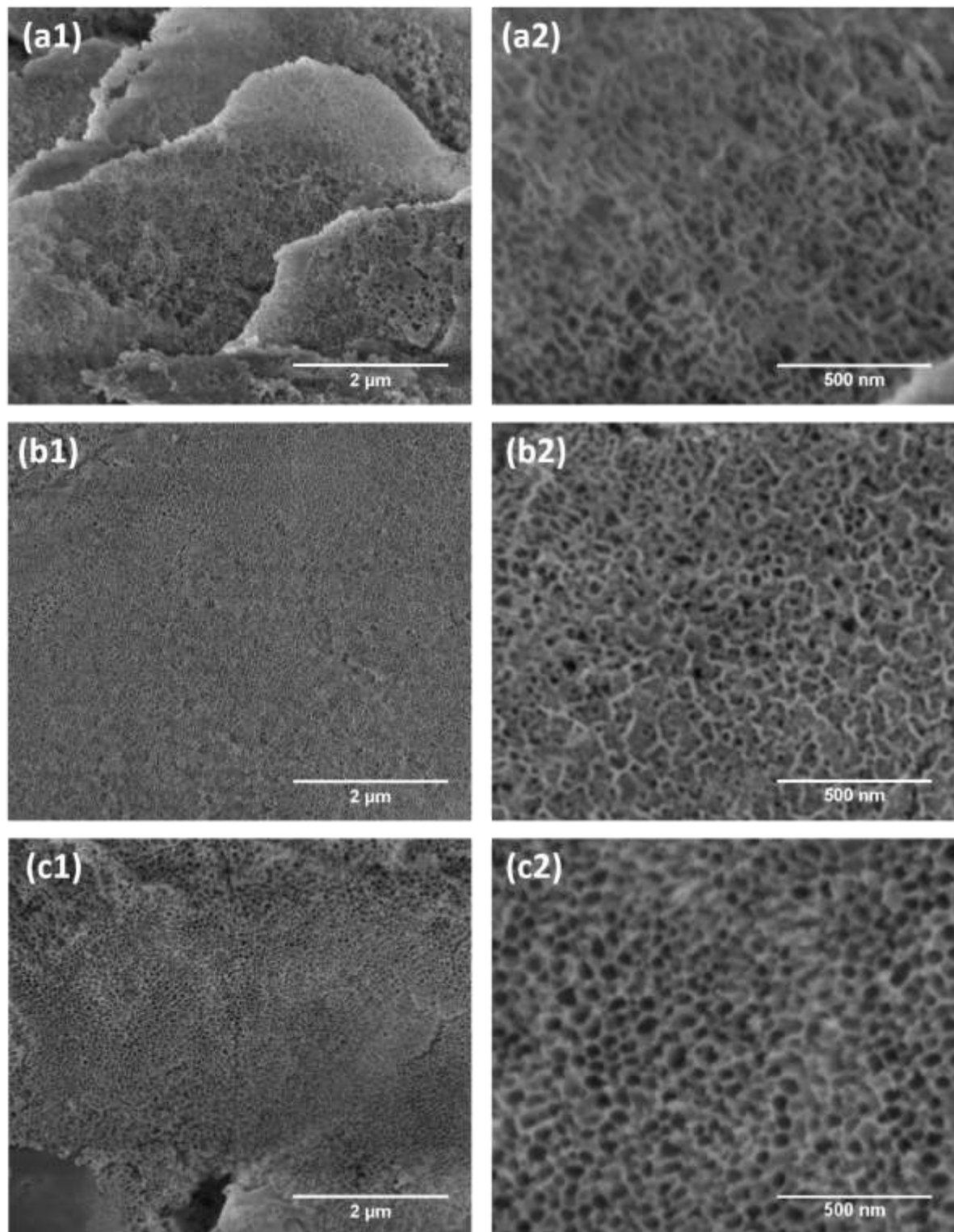
pores inside larger pores.

Figure 5. Top-view FEGSEM micrographs of the Ta nanostructured surface development by (a) two-steps anodization (Ta-anod5), (b) one-step anodization for 60 minutes (Ta-anod6) and (c) 2.4 wt.% NH₄F in ES electrolyte for 20 minutes (Ta-anod7). (a1, b1, c1): surface morphology of anodized samples and (a2, b2, c2) their respectively high magnification.

In general terms, the two-step anodization produced patchy anodic layers with less-ordered nanostructured surfaces in comparison to one-step anodization, reason why the two-step approach was not further considered on this work.

The obtained morphology of sample Ta-anod6 could suggest that, under these conditions, the 20 minutes (Ta-anod4 sample) process duration was not enough to develop a nanostructured anodic film with nanostructure. Thus, one possibility would be increasing the process duration, however this would not be viable, since the current over 60 min was too high, showing a rapid increase (see Figure 2~~Figure 2~~-c and d) . Thereby, in order to increase the dissolution rate with controllable current density, one-step anodization was performed for 20 min raising the concentration of NH_4F to 2.4 wt.% on ES (Ta-anod7 in Table 1~~Table 1~~). Under these conditions, it was possible to obtain a more uniform porous structure, Figure 5~~Figure 5~~-c (c1 andc2). In Figure 2~~Figure 2~~-a (or b) the current density-time curve shows a long second stage, exhibiting a continued increase in current density with fast periodic oscillations, but not reaching a steady-state. The increase of current density is associated with the accelerated dissolution of the anodic layer, due to the high concentration of NH_4F. Notice also the strong increase in electrolyte temperature, related to the strong current flow through the oxide layer, which further accelerates chemical dissolution, due to the enhancement of chemical reaction rates. This increase in eletrolyte temperature leads not only to an unbalance between oxide formation/dissolution kinetics, explaining the continuous increase of current density, but also to an increase in ion diffusion in electrolyte, while at the same time introduces turbulence in the mass transport. A similar behaviour of eletrolyte temperature was previously observed in Ta anodization performed under RT, recording at the third stage some oscillations in current density curve which was attributed to an increase in the solution conductivity as the solution temperature increased 3°C in 10 min, for a higher HF concentration at the

electrolyte [31]. Nevertheless, it is not possible to compare the overall current density-time curves experimentally obtained in this work with the reported in the literature since the current densities recorded are almost one hundred times order of magnitude superior. Only the curve behavior for the initial times (Figure 2Figure 3-a and b insets) are in the same order of magnitude.

The high current density could also lead to acidification of the electrolyte and accompanied by abundant gas production, due to water hydrolysis [19], [38]:

$$2H_2O \rightarrow O_2 + 4H^+ + 4e^- \tag{3}$$
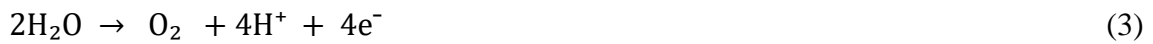
In this sense, pH of electrolyte was measured before and after anodization, 5.6 and 4.8 respectively. Anodizing for longest time, could contribute to the acidic dissolution and consequently inducing a merging the neighboring pores [46], [49]. The joint action of all these factors explains the observed random nanoporous morphology, due to disordered grow of porous in the oxide layer [45].

An interesting feature in current density curve is the presence of fast current oscilations for high NH_4F concentration, as shown in Figure 2Figure 2-a (or b). This oscilations started to occur at second stage and could be the result of the breakdown on the oxide-metal interface. In literature, current (or voltage) oscillations are reported during anodization of several metals, as Si [V. Parkhutik, J. Curiel-Esparza, M.-C. Millan, J. Albella, Phys. Status Solidi A 2005, 202, 1576[lm1]], Ti [40-42] or Al [46], and numerous models were suggested. For Si,Ti voltage oscillations were ascribed to the alternating stages of anodic oxide growth and lifting-off, while in case of Al, the current oscillations were attributed to the oxidation process controlled by electrolyte diffusion through the pore combined with the local heat generation, due to the exothermic nature of the oxidation reaction.

Therefore, as the more uniform porous structure achieved was the sample produced by one-step anodization under 60V with an electrolyte of 2.4 wt.% NH_4F in ES for 20 min, Ta-anod7 sample was further characterized.

3.2. Oxide structure and thickness

In order to to study the morphology of produced anodic layers the cross-section of the sample Ta-anod7 was analyzed (Figure 6Figure 5). The anodic layer nanostructure consists in multiple thin and porous layers instead of a columnar structure with pores. Moreover, the thickness of the anodic layer was around 5.3 µm, which, according to the literature, fits in the range 4-16 µm of Ta porous layer thickness under different electrochemical conditions using non-aqueous electrolytes with NH_4F [24]. Identic multiple layers were obtained by Ta anodization for 120 min in 1 M H_2SO_4 and 3.3 wt.% NH_4F at 20 V, showing that every layer exhibited a closed bottom, but any further explanation was discussed [37]. Multiple thin discontinuous porous layers on Ta substrate formed by one-step anodization were associated, in literature, to the requirement of lower water content (or higher fluoride concentration) in the electrolyte to achieve this morphology [24]. H. Yu et al. [34] reported that the coral-like nanoporous structure formation is water-content sensitive and is only obtained when dissolution rate was not enough to form pores/ pits on the surface meaning low fluoride ions concentration. However, for Ti-based materials it was demonstrated that a minimum content of water in

EG electrolyte was necessary to obtain well-order Ti nanotubes which should not exceed a critical limit, otherwise local pH condition was affected and there were formation of ridges on the nanotubes [47]. Apart from the electrolyte concentration, formation of thin oxide Ta multilayers could be related to higher potentials and high dissolution current [19]. When the applied voltage is too high, loosely-connected layers were formed [24].

As previous discussed, the current density-time curve recorded, Figure 2Figure 2-a (or b), doesn't exhibit a typical behavior neither typical values (higher than literature). . The voltage(current) oscillatory behaviors during the anodization in case of titanium or silicon has been attributed to a cyclic process of growth and detachment of anodic oxides forming a stack of oxide layers [41],[V. Parkhutik, J. Curiel-Esparza, M.-C. Millan, J. Albella, Phys. Status Solidi A 2005, 202, 1576].

For Si, the mechanism proposed for layer detachment is based on accumulation of mechanical stress at the oxide/Si interface, that further triggers isotropic etching of multiple pores. For Ti anodization, they were ascribed to periodical undermining of the ordered nanotubular layer when the voltage exceeded certain values. Moreover, stress effects related to the mismatch of the oxide and substrate, which could lead to cracking at the metal/oxide interface, were previously reported in Ta anodization [19].
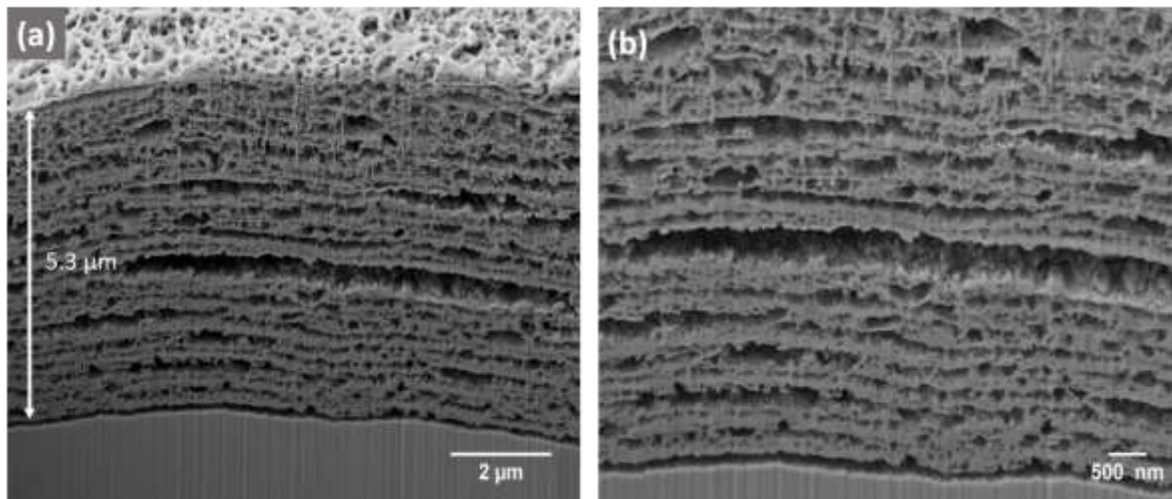

Figure 6. SEM images of the FIB cross-sections of Ta-anod7 sample at (a) lower and with (b) higher magnification.

Apart from the multiple thin anodic layers (Figure 6Figure 6), a continuous interface between Ta substrate and anodic layer is clearly observed. This is likely to be a hollow

space, indicating a lift-off of the anodic layer from the substrate. Similar interface was reported in Ti anodization having a hollow space between Ti and titania nanotubes [15]. A mechanism has been proposed for anodic layer detachment in Ti anodization, namely water assisted dissolution of the fluoride-rich layer in the interface of metal/oxide. It has been widely accepted that this layer enriched with fluoride formation can be ascribed to the twice migration rate of F^- comparing with O^{2-} ions for aqueous electrolytes [30]. Thus, the interfacial hollow space could be related to the dissolution of the fluoride-rich layer after immersion in containing-water solutions [15], for instance during the rinse of the samples with distillated water. Likewise, a tantalum-fluoride complex could be formed [29], Eq.2, resulting in the build-up of fluoride-rich layer (likely TaF_5) at Ta/Ta_2O_5 interface which could cause the detach of the anodic layer form the Ta surface [28], [31].

The observed layering effect is surprisingly similar with that of regular oscillations of anodic potential during Si anodization in very diluted HF [V. Parkhutik, Solid-State Electron. **45**, 1451 (2001)]. The periodic formation of porous layers and their lift-off from the substrate was explained, in terms of periodic change of intensity and anisotropy of electrochemical dissolution reaction and accumulation of mechanical stress within growing Ta2O5 layer. The layering of the growing film might be associated with fluctuations of local current density at the pore bottoms associated with accumulation and release of gas bubbles from the surface of the sample. The gas bubbles growing at the surface, mask part of the surface, preventing the increase or even reducing the local current density. When the bubble leaves the surface, current density in the pores jumps back to steady-state level with simultaneous change of the intensity of electrochemical reactions contributing to the formation porous layer. The accumulation of gas bubbles at the pores can develop very high internal pressure which are able to provoke a collapse of the porous layer and trigger the lift-off of the mechanically stressed Ta_2O_5 oxide layer.

In order to reduce the stress mismatch effect at the metal/anodic oxide interface, a surface electropolishing was performed as pre-treatment to form a compact Ta oxide what was then used as substrate for anodization, Figure 1Figure 1-b. In this way, anodization starting point was already oxidized surface with similar properties. Yet, it is not completely evident that this stress effect in the interface is the main factor for the

delamination process, because the layer stacking is still observed in sample anodized after the pre-treatment. The most reliable explanation possibility must be related to the gas formation and evolution as the main mechanism responsible for triggering the layer's delamination and especially for the gaps between them, due the high internal gas pressure developed..

3.3. Phase composition

XRD analyses was carried out in order to understand the evolution of the structure caused by the topographic, morphologic and chemical modifications of the Ta substrate during anodization. <u>Figure 7</u>~~Figure 7~~ presents the diffraction patterns for Ta sheet before any treatment, Ta-pol and Ta-anod. The main crystalline phases identified are α-Ta: body-centered cubic (bcc) (ICDD card n. 00-004-0788) and β-Ta: tetragonal (ICDD card n. 00-025-1280).

Ta sheet presented a mixture of both α-Ta and β-Ta phases. The presence of α-Ta and β-Ta phases in both Ta-pol and Ta-anod samples was related with the crystalline composition of the base material, Ta sheet. The absence of any further diffraction peak indicated that Ta_2O_5 anodic layer was amorphous, barely observed in Ta-anod pattern for lower angles, consistent with previous studies [26]. Similar results were also observed by Momeni et. al [32] where Ta anodized exhibited diffraction peak of Ta substrate and after annealing at 400°C the sample revealed new diffraction peaks, with a low intensity, of

crystalline Ta_2O_5. Gonçalves et al. [48] demonstrated that thermal treatment above 750°C result in crystalline structure formation with Ta_2O_5 orthorhombic phase appearing. Also, it was evident that the dissolution rate has an important influence on the sheet orientations. Before any treatment, it was noticed that Ta sheet presented a preferential orientation in the [211] direction. After the electrochemical process, the [211] direction was consumed and a preferential [110] direction arose. The results revealed that the high atomic packing for (211) planes allowed a higher dissolution rather than the (110) planes which reveled more resistance to be consumed during anodization. Moreover, Chen et al. exposed [26] the idea that the grain size and orientation of Ta substrate can affect the patchy structure of nanotube arrays. In addition, El-Sayed et al. [29] proposed a different etch speed as function of the crystallographic orientation of Ta grains. For that, the authors studied the anodized Ta surface morphology of the same sample for three different grains and the morphologies were not identical to each other suggesting a differential etching for each grain. Although these reported Ta anodizations were carried out using aqueous electrolytes, the presence of distinct morphologies and inhomogeneity (regions with more pores, larger pores and smoother areas) on the anodic surface, Figure 3Figure 2, can be related to the different dissolution/ oxidation rates induced by the different orientation crystals along Ta sheet.
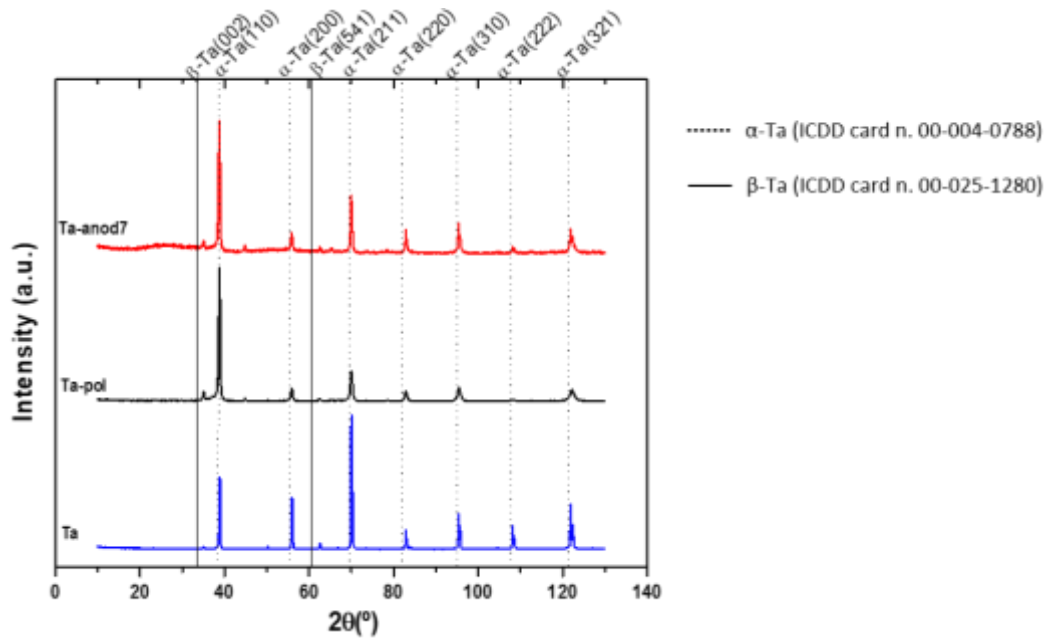
Figure 7. XRD diffractograms of Ta sheet without any treatment (Ta - blue row); Ta with pre-treatment (Ta-pol - black row) and Ta anodized (Ta-anod7 - red row).

3.4. Chemical composition

The EDS spectra acquired from Ta-pol and Ta-anod were shown Figure 8Figure 8-a and b, respectively, where is observed that with the surface pre-treatment, Ta element was detected such as a residual amount of Carbon (C) and some Oxygen (O) due to the tantalum oxidation expected by electropolishing. After anodization process, beyond the mentioned elements, Fluorine (F) was also detect on the surface of Ta-anod with an increasing of O content, which was likely related with the increase of the anodic layer thickness. Chemical composition depicted in **Error! Reference source not found.**Table 2.
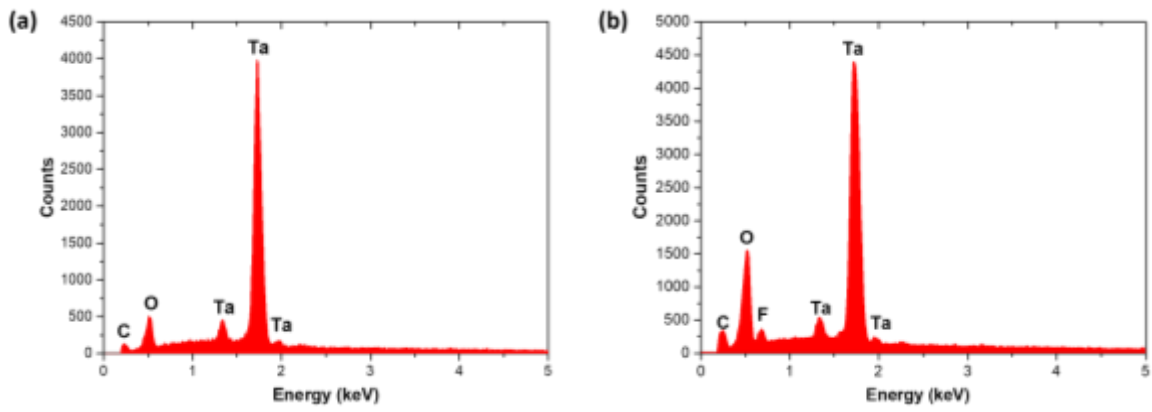
Figure 8- EDS spectra of (a) Ta-pol and (b) Ta-anod7 samples.

Considering that EDS technique analyses the materials composition in depth, to have a more reliable and accurate measurement of the surface chemical composition XPS analysis was performed on both sample surfaces. In Figure 9Figure 9 a is displayed both surveys and quantitative results are summarized in **Error! Reference source not found.**Table 2. The chemical composition of both surfaces is similar, a part of the fact that in Ta-pol sulfur (S) contamination was detected, which came from the electrochemical polishing with H_2SO_4.

Table 2. Chemical composition of Ta-pol and Ta-anod samples by EDS and XPS.

Sample	Chemical composition (at. %)					
	EDS			XPS		
	Ta	O	F	Ta 4f	O 1s	F 1s
Ta-pol	60 ± 0.6	38 ± 2.3	-	26.99	73.01	-
Ta-anod7	35 ± 0.6	58 ± 1.2	6.2 ± 4.5	17.87	73.02	9.12

These findings can indicate that S element is present on the top layer of the oxide or its content is too low, and, because of that, it was only detected by XPS and not by EDS. This contamination was also noticed by Namur et al. [21] in compact Ta_2O_5 obtain in 1 M H_2SO_4 anodization. In Ta-anod7, the F peak appeared due to the used electrolyte during anodizing process. Chemical quantification by XPS revealed higher O content and lower Ta content because the surface was oxidized. Moreover, Ta 4f doublet (Figure 9Figure 9-b) corresponded to Ta^{5+} in Ta_2O_5 [50] for both Ta-pol and Ta-anod7 samples with peak binding energies for Ta $4f_{7/2}$ at 26.5 eV and 26.3 eV, respectively, and the metallic state was not detected (the Ta^0 $4f_{7/2}$ peak would be detected at 21.5 eV [51]). While the dissolution reaction is continuously occurringa fluoride-rich Ta_2O_5 layer builds-up at the metal/oxide interface and remaining on surface after oxide film detachment [28]. Nevertheless, in this study, no evidence of TaF_5 was found, which would be expected at 27.8 eV [19]. However, a binding energy peak around 685 eV was detected, which corresponds to F 1s. Its presence has been reported on Ti nanostructured surfaces obtained by anodization with a mixture of EG, H_2O and NH_4F electrolyte, being attributed toadsorbed F^- ions [52]–[54]. It is thus reasonable to assumed that the F 1s peak detected corresponds to F^- ions adbsorbed on Ta_2O_5. Furthermore, it is possible that fluoride-rich layer is dissolved after the lift-off, resulting in the re-precipitatation of a salt layer on to the growing porous oxide surface.

4. Conclusion

In this work it was shown the possibility to develop a nanostructure on Ta oxide layer using a non-aqueous and acid-free electrolyte composed only by an organic solvent, EG, and water. Addition of different content of NH_4F affected the nanostructure and current density-time curve recorded during anodizing process. A more concentrated electrolyte led to an increasing current density, and a nanostructure was obtained. However, these anodization conditions ascribed to a more unstable variation of the current density with time, and a different behavior of the typical anodization current-time curve with a magnitude 100 times higher than the conventional. Under these conditions, the

electrochemical oxide dissolution was harder, leading toa strong increase electrolyte temperature, and consequently in an unbalance between dissolution and oxide formation rates, preventing the current density from achieving the steady-state. Under this conditions, a porous nanostructure, quite organized and homogenous, was formed, however under very unstable conditions. FIB/SEM cross-sectional images revealed a multi-layered structure, consisting in a stacking of thin porous layers, due to layer lift-off triggered by the gas accumulation and subsequent release at interface substrate/oxide layer during the anodization. Furthermore, two-step anodization efforts to improve adhesion of the oxide layer did not show any morphology improvement comparing with one-step anodization using a non-aqueous electrolyte.

Acknowledgements

References

[1]   S. Minagar, C. C. Berndt, J. Wang, E. Ivanova, and C. Wen, "A review of the

application of anodization for the fabrication of nanotubes on metal implant surfaces," *Acta Biomater.*, vol. 8, no. 8, pp. 2875–2888, 2012.

[2]   X. Liu, P. K. Chu, and C. Ding, "Surface modification of titanium, titanium alloys, and related materials for biomedical applications," *Mater. Sci. Eng. R Reports*, vol. 47, no. 3–4, pp. 49–121, 2004.

[3]   S. E. Kim, J. H. Lim, S. C. Lee, S. C. Nam, H. G. Kang, and J. Choi, "Anodically nanostructured titanium oxides for implant applications," *Electrochim. Acta*, vol. 53, no. 14, pp. 4846–4851, 2008.

[4]   J. M. Macak *et al.*, "TiO2 nanotubes: Self-organized electrochemical formation, properties and applications," *Curr. Opin. Solid State Mater. Sci.*, vol. 11, no. 1–2, pp. 3–18, 2007.

[5]   T. J. Webster and C. Yao, "Anodization: A promising nano modification technique of titanium-based implants for orthopedic applications," in *Surgical Tools and Medical Devices, Second Edition*, 2016.

[6]   M. J. Jackson and W. and Ahmed, "Chapter 2 Anodization : A Promising Nano-Modification Technique of Titanium-based Implants for Orthopedic Applications," in *Surface Engineered Surgical Tools and Medical Devices*, Boston, MA: Springer US, 2007, pp. 21–47.

[7]   B. Ercan, E. Taylor, E. Alpaslan, and T. J. Webster, "Diameter of titanium nanotubes influences anti-bacterial efficacy," *Nanotechnology*, vol. 22, no. 29, p. 295102, 2011.

[8]   X. Yu, Y. Li, W. Wlodarski, S. Kandasamy, and K. Kalantar-zadeh, "Fabrication of nanostructured TiO2 by anodization: A comparison between electrolytes and substrates," *Sensors Actuators, B Chem.*, vol. 130, no. 1, pp. 25–31, 2008.

[9]   F. Rupp, L. Liang, J. Geis-Gerstorfer, L. Scheideler, and F. Hüttig, "Surface characteristics of dental implants: A review," *Dent. Mater.*, vol. 34, no. 1, pp. 40–57, 2018.

[10]   Q. Lu *et al.*, "Anodic film growth on tantalum in dilute phosphoric acid solution at 20 and 85°C," *Electrochim. Acta*, vol. 47, pp. 2761–2767, 2002.

[11]   Z. B. Yang, J. C. Hu, K. Q. Li, S. Y. Zhang, Q. H. Fan, and S. A. Liu, "Advances of the research evolution on aluminum electrochemical anodic oxidation technology," *IOP Conf. Ser. Mater. Sci. Eng.*, vol. 283, no. 1, pp. 0–14, 2018.

[12]   P. Roy, S. Berger, and P. Schmuki, "TiO2 Nanotubes : Synthesis and Applications," *Angew. Chem. Int*, vol. 50, pp. 2904–2939, 2011.

[13]   H. A. El-Sayed, C. A. Horwood, A. D. Abhayawardhana, and V. I. Birss, "New insights into the initial stages of Ta oxide nanotube formation on polycrystalline Ta electrodes," *Nanoscale*, vol. 5, no. 4, pp. 1494–1498, 2013.

[14]   S. P. Rodrigues, C. F. A. Alves, A. Cavaleiro, and S. Carvalho, "Water and oil wettability of anodized 6016 aluminum alloy surface," *Appl. Surf. Sci.*, vol. 422, pp. 430–442, 2017.

[15]   S. A. Alves *et al.*, "A first insight on the bio-functionalization mechanisms of TiO2 nanotubes with calcium, phosphorous and zinc by reverse polarization anodization," *Surf. Coatings Technol.*, vol. 324, no. May, pp. 153–166, 2017.

[16]   S. M. F. Carvalho and C. F. A. Alves, "Dental implant," WO2016042515 A1, 2016.

[17]   Y. Fu and A. Mo, "A Review on the Electrochemically Self- organized Titania Nanotube Arrays : Synthesis , Modifications , and Biomedical Applications," *Nanoscale Res. Lett.*, vol. 13, pp. 2–21, 2018.

[18]   K. Prasad *et al.*, "Metallic Biomaterials : Current Challenges and Opportunities," *Materials (Basel).*, vol. 10, no. 8, p. 884, 2017.

[19]   I. V. Sieber and P. Schmuki, "Porous Tantalum Oxide Prepared by Electrochemical Anodic Oxidation," *J. Electrochem. Soc.*, vol. 152, no. 9, p. C639, 2005.

[20]   M. Sowa *et al.*, "Influence of process parameters on plasma electrolytic surface treatment of tantalum for biomedical applications," *Appl. Surf. Sci.*, vol. 407, pp. 52–63, 2017.

[21]   R. Sanson, K. Miriam, C. Eliana, and B. Marino, "Growth and Electrochemical Stability of Compact Tantalum Oxides Obtained in Different Electrolytes for Biomedical Applications," *Mater. Res.*, vol. 18, no. Suppl 2, pp. 0–6, 2015.

[22]   D. Cristea, I. Ghiuță, and D. Munteanu, "Tantalum based materials for implants and prosthesis applications," *Bull. Transilv. Univ. Braşov*, vol. 857, no. 2, 2015.

[23]   C. F. Almeida Alves, A. Cavaleiro, and S. Carvalho, "Bioactivity response of Ta1-xOx coatings deposited by reactive DC magnetron sputtering," *Mater. Sci. Eng. C*, vol. 58, pp. 110–118, 2016.

[24]   W. Wei, J. M. Macak, and P. Schmuki, "High aspect ratio ordered nanoporous Ta2O5 films by anodization of Ta," *Electrochem. commun.*, vol. 10, no. 3, pp. 428–432, 2008.

[25]   W. Wei, J. M. Macak, N. K. Shrestha, and P. Schmuki, "Thick Self-Ordered Nanoporous Ta2O5 Films with Long-Range Lateral Order," *J. Electrochem. Soc.*, vol. 156, no. 6, p. K104, 2009.

[26]   W. Chen *et al.*, "Study on morphology evolution of anodic tantalum oxide films in different using stages of H2SO4/HF electrolyte," *Electrochim. Acta*, vol. 236,

pp. 140–153, 2017.

[27]   H. El-Sayed, S. Singh, M. T. Greiner, and P. Kruse, "Formation of highly ordered arrays of dimples on tantalum at the nanoscale," *Nano Lett.*, vol. 6, no. 12, pp. 2995–2999, 2006.

[28]   H. A. El-Sayed and V. I. Birss, "Controlled interconversion of nanoarray of Ta dimples and high aspect ratio Ta oxide nanotubes," *Nano Lett.*, vol. 9, no. 4, pp. 1350–1355, 2009.

[29]   H. El-Sayed, S. Singh, and P. Kruse, "Formation of Dimpled Tantalum Surfaces from Electropolishing," *J. Electrochem. Soc.*, vol. 154, no. 12, p. C728, 2007.

[30]   N. K. Allam, X. J. Feng, and C. A. Grimes, "Self-Assembled Fabrication of Vertically Oriented Ta2O5 Nanotube Arrays , and Membranes Thereof , by One-Step Tantalum Anodization," *Chem. Mater.*, vol. 20, pp. 6477–6481, 2008.

[31]   H. A. El-Sayed and V. I. Birss, "Controlled growth and monitoring of tantalum oxide nanostructures," *Nanoscale*, vol. 2, no. 5, pp. 793–798, 2010.

[32]   M. M. Momeni, M. Mirhosseini, and M. Chavoshi, "Fabrication of Ta2O5 nanostructure films via electrochemical anodisation of tantalum," *Surf. Eng.*, vol. 0844, no. July, p. 160226022403003, 2015.

[33]   Y. Kado, R. Hahn, C. Y. Lee, and P. Schmuki, "Strongly enhanced photocurrent response for Na doped Ta3N5-nano porous structure," *Electrochem. commun.*, vol. 17, no. 1, pp. 67–70, 2012.

[34]   H. Yu, S. Zhu, X. Yang, X. Wang, H. Sun, and M. Huo, "Synthesis of Coral-Like Tantalum Oxide Films via Anodization in Mixed Organic-Inorganic Electrolytes," *PLoS One*, vol. 8, no. 6, pp. 6–11, 2013.

[35] K. Lee and P. Schmuki, "Highly ordered nanoporous Ta2O5 formed by anodization of Ta at high temperatures in a glycerol/phosphate electrolyte," *Electrochem. commun.*, vol. 13, no. 6, pp. 542–545, 2011.

[36] M. Sarraf *et al.*, "Nanomechanical properties, wear resistance and in-vitro characterization of Ta2O5 nanotubes coating on biomedical grade Ti–6Al–4V," *J. Mech. Behav. Biomed. Mater.*, vol. 66, no. August 2016, pp. 159–171, 2017.

[37] S. Minagar, C. C. Berndt, and C. Wen, "Fabrication and characterization of nanoporous niobia, and nanotubular tantala, titania and zirconia via anodization," *J. Funct. Biomater.*, vol. 6, no. 2, pp. 153–170, 2015.

[38] I. Sieber, H. Hildebrand, A. Friedrich, and P. Schmuki, "Initiation of tantalum oxide pores grown on tantalum by potentiodynamic anodic oxidation," *J. Electroceramics*, vol. 16, no. 1, pp. 35–39, 2006.

[39] X. Wang, S. Zhang, and L. Sun, "A Two-step anodization to grow high-aspect-ratio TiO2 nanotubes," *Thin Solid Films*, vol. 519, no. 15, pp. 4694–4698, 2011.

[40] S. Chen, M. Liao, P. Yang, S. Yan, R. Jin, and X. Zhu, "Simulation of anodizing current-time curves and the morphology evolution of TiO2nanotubes obtained in phosphoric electrolytes," *RSC Adv.*, vol. 6, no. 87, pp. 84309–84318, 2016.

[41] L. V Taveira, J. M. Macak, K. Sirotna, L. F. P. Dick, and P. Schmuki, "Voltage Oscillations and Morphology during the Galvanostatic Formation of Self-Organized TiO2 Nanotubes," *J. Electrochem. Soc.*, vol. 153, no. 4, pp. 137–143, 2006.

[42] W. Z. Shen, "Controllable current oscillation and pore morphology evolution in the anodic growth of TiO2," *Nanotechnology*, no. 22, pp. 1–12, 2011.

[43] K. Indira, U. K. Mudali, T. Nishimura, and N. Rajendran, "A Review on TiO2

Nanotubes: Influence of Anodization Parameters, Formation Mechanism, Properties, Corrosion Behavior, and Biomedical Applications," *J. Bio- Tribo- Corrosion*, vol. 1, no. 4, pp. 1–22, 2015.

[44]   D. Khudhair *et al.*, "Anodization parameters influencing the morphology and electrical properties of TiO 2 nanotubes for living cell interfacing and investigations," *Mater. Sci. Eng. C*, vol. 59, pp. 1125–1142, 2016.

[45]   A. Ghicov and P. Schmuki, "Self-ordering electrochemistry: A review on growth and functionality of TiO2 nanotubes and other self-aligned MOx structures," *Chem. Commun.*, no. 20, pp. 2791–2808, 2009.

[46]   B. W. Lee, J. Kim, and U. Go, "Spontaneous Current Oscillations during Hard Anodization of Aluminum under Potentiostatic Conditions," *Adv. Funct. Mater.*, vol. 20, pp. 21–27, 2010.

[47]   K. S. Raja, T. Gandhi, and M. Misra, "Effect of water content of ethylene glycol as electrolyte for synthesis of ordered titania nanotubes," *Electrochem. commun.*, vol. 9, no. 5, pp. 1069–1076, 2007.

[48]   R. V. Gonçalves *et al.*, "Ta2O5 nanotubes obtained by anodization: Effect of thermal treatment on the photocatalytic activity for hydrogen production," *J. Phys. Chem. C*, vol. 116, no. 26, pp. 14022–14030, 2012.

[49]   T. Aerts, T. Dimogerontakis, I. De Graeve, J. Fransaer, and H. Terryn, "Influence of the anodizing temperature on the porosity and the mechanical properties of the porous anodic oxide film," *Surf. Coatings Technol.*, vol. 201, no. 16–17, pp. 7310–7317, 2007.

[50]   J. Y. Zhang and I. W. Boyd, "Thin tantalum and tantalum oxide films grown by pulsed laser deposition," *Appl. Surf. Sci.*, vol. 168, no. 1–4, pp. 234–238, 2000.

[51] R. Simpson, R. G. White, J. F. Watts, and M. A. Baker, "XPS investigation of monatomic and cluster argon ion sputtering of tantalum pentoxide," *Appl. Surf. Sci.*, vol. 405, pp. 79–87, 2017.

[52] S. A. Alves *et al.*, "Synthesis of calcium-phosphorous doped TiO2 nanotubes by anodization and reverse polarization: A promising strategy for an efficient biofunctional implant surface," *Appl. Surf. Sci.*, vol. 399, no. December, pp. 682– 701, 2017.

[53] S. C. Han *et al.*, "Highly Ordered Self-Organized TiO 2 Nanotube Arrays Prepared by a Multi-Step Anodic Oxidation Process," vol. 15, no. 3, pp. 493– 499, 2009.

[54] R. P. Antony, T. Mathews, S. Dash, A. K. Tyagi, and B. Raj, "X-ray photoelectron spectroscopic studies of anodically synthesized self aligned TiO2 nanotube arrays and the effect of electrochemical parameters on tube morphology," *Mater. Chem. Phys.*, vol. 132, no. 2–3, pp. 957–966, 2012.